AD-A045 662 GENERAL ELECTRIC CO SYRACUSE N Y HEAVY MILITARY ELEC--ETC F/G 17/1
DETECTABILITY OF LINEAR FM PULSES TRANSMITTED THROUGH A RANDOM --ETC(U)
1966 S M GARBER

UNCLASSIFIED NL

| OF |
AD
A045662

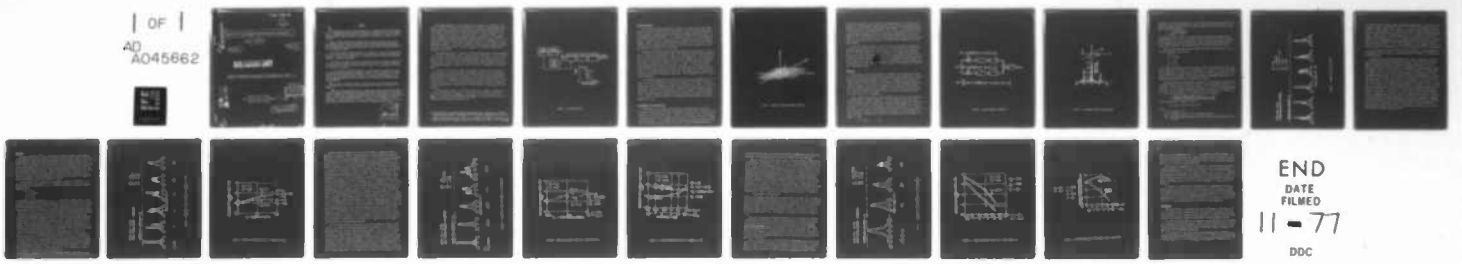

END
DATE
FILMED
11-77
DDC

DETECTABILITY OF LINEAR FM PULSES TRANSMITTED THROUGH A RANDOM MEDIUM

by

S. M. Garber

1966

24 p.

Presented at NATO-Marina Italiana Advanced Study Institute on Stochastic Problems in Underwater Sound Propagation, 18-23 September 1967, Lerici, Italy

General Electric Company
Heavy Military Electronics ~~Department~~ System
Syracuse, New York 13201

ABSTRACT

The objective of the work to be described is to determine some of the implications of medium distortion on waveform and processor design for active echo-ranging sonar. In particular, the questions of bandwidth and duration of linear FM signals are considered, as well as various combinations of coherent and incoherent processing.

Sonar echos are modeled as a multiplicity of discrete arrivals, the arrival time (range), doppler shift and amplitude being chosen at random from specified probability densities. Noise is modeled as white with gaussian amplitude statistics, and reverberation as having gaussian amplitude statistics but the power spectrum of the transmitted signal.

With these models, computer simulation is employed to examine the detectability of echos produced by the transmission of linear FM pulses of various bandwidths and durations. The processor consists of a correlator followed by various amounts and shapes of incoherent integration.

Monte Carlo techniques are used to generate ROC curves, showing the probability of an echo being detected on a given ping vs the probability of a false detection in the absence of an echo, with input signal-to-noise ratio or signal-to-reverberation ratio as a parameter.

It is shown that, when the background is predominantly reverberation, in spite of severe time spreading of echos significant gains in detection are still attainable through the use of extreme bandwidths. There is an accompanying loss in detection, of the wider band signals compared to the narrower band signals, with a noise background. This loss is less, however, than the gain achieved when reverberation limited.

The conclusion reached from these results is that best detection performance is obtained by use of a pulse with as much bandwidth as system constraints will permit.

It is also shown that post detection integration, following coherent processing, sometimes improves detectability, and sometimes degrades detectability, depending on the "denseness" of the multipath compared to the time resolution of the transmitted signal. If the signal energy is divided between a few widely spaced arrivals, such as might result from an extended target, it is better not to integrate. On the other hand, if the spread is more or less continuous, such as could occur by reflection from the surface or bottom, it is better to integrate over the spread.

The primary purpose of the work reported in this paper is to evaluate, using computer simulation techniques, the performance of linear frequency modulated active sonar signals and processors in a randomly fluctuating medium. This problem has been treated by Price and Green[1] and by this author in a previous paper[2]. In both cases, range-doppler spreading was assumed uniform and constant. In this paper, range and doppler spreading are treated as random variables in order to more closely represent the conditions that signals actually encounter in the underwater acoustic operating environment. In general, spreading is introduced by the target, the medium and the echo ranging platform. These are combined in the single spreading model employed in this study.

Echo energy splitting is treated as a stationary random process whose parameters can be varied to study their effect on detectability of LFM echos. It will be shown that, at least for the energy splitting models assumed, the LFM pulse holds up exceedingly well, and that, in most sonar applications, system constraints rather than the propagating medium or target, will limit the choice of transmitted pulse bandwidth.

In order to carry out this study, the signals, the noise, and the processor were simulated on a computer and Monte Carlo methods used to obtain the processor output statistical quantities of probability of false alarm (PFA) and probability of detection (PD). Comparisons are then made on the basis of required input signal-to-interference ratio (SIR) to produce a specified value of PD when a threshold is set for a specified PFA. Figure 1 shows a block diagram of the processes that are simulated.

The discussion to follow is divided into four parts. First - a discussion of the energy splitting model; second - a brief mention of the interference model; third - a description of the processor; and fourth - the results that have been obtained and the conclusions they have led to.

---

1. Price and Green, "Signal Processing in Radar Astronomy - Communication via Fluctuating Multipath Media", Tech. Report No. 234, Lincoln Laboratory, MIT, 6 Oct. 1960.
2. Garber, "High Resolution Sonar Signals in a Multipath Environment", Supplement to IEEE Transactions on Aerospace and Electronic Systems, Vol. AES-2, No. 6, Nov. 1966.

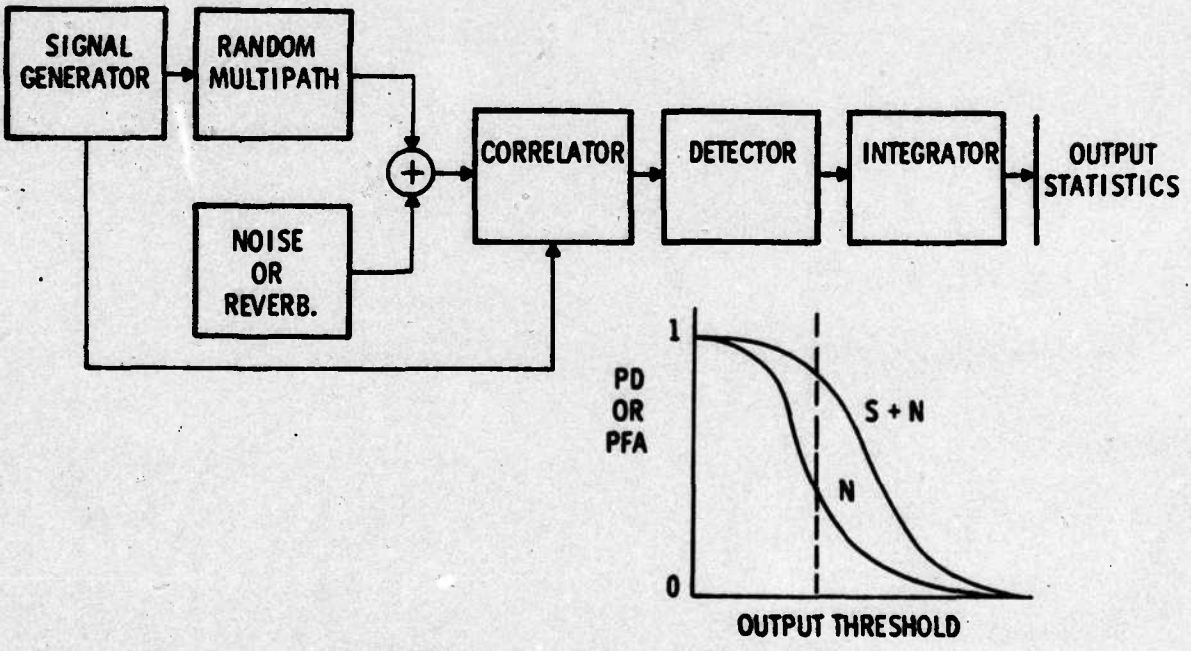

FIGURE 1. SIMULATION MODEL

TARGET ECHO MODEL

The choice of signal spreading model is difficult because insufficient experimental data exists on which to base a good model. The model that has been adopted for this study is a highly flexible one which was originally developed by the U. S. Navy Underwater Sound Laboratory. It is intended to account for the spreading that could occur upon reflection from the surface or bottom and to account for extended targets. There are certain non-random multipath modes, such as the surface triplet associated with a target below the surface or any fixed echo structure of the target that are not accounted for in this model.

The model assumes that the received signal energy is divided among a multiplicity of replicas of the transmitted signal, each replica or arrival having associated with it a particular range delay τ_i, doppler ϕ_i, and amplitude a_i. For a given echo the total received energy is equal to the sum of the energies in all of the individual arrivals. Figure 2 illustrates the idea. It shows the range delay, doppler shift and amplitude of each of six arrivals in one echo. It is assumed that the time variations of the target and path are slow enough that range, doppler and amplitude do not change during a pulse length, but fast enough that their values from one ping to the next are completely independent. These assumptions seem to be borne out by experience.

It is further assumed that the variables within a ping are independent of each other. Hence, the amplitude of a path does not depend on its position in range or doppler, nor does the doppler shift depend on time delay, etc. Thus, τ, ϕ and a are independent, stationary random variables. Range delay is assumed normally distributed about a mean $\overline{\tau}$ with a standard deviation of σ_τ seconds. Similarly, doppler shift is assumed normally distributed about zero mean with a standard deviation of σ_ϕ Hz. Finally, energy is assumed to be log-normally distributed with a standard deviation of σ_a db.

REVERBERATION AND NOISE MODEL

Reverberation is the summation of echos from a multiplicity of scatterers. Therefore, the same model with different parameters could be used to represent reverberation as is used for target echos. However, in this study we have been primarily concerned with the effects of target echo distortion, and hence, have used a simpler reverberation model. It is assumed that the scatterers are closely spaced, and randomly distributed in range and angle, and that the average scattering strength is

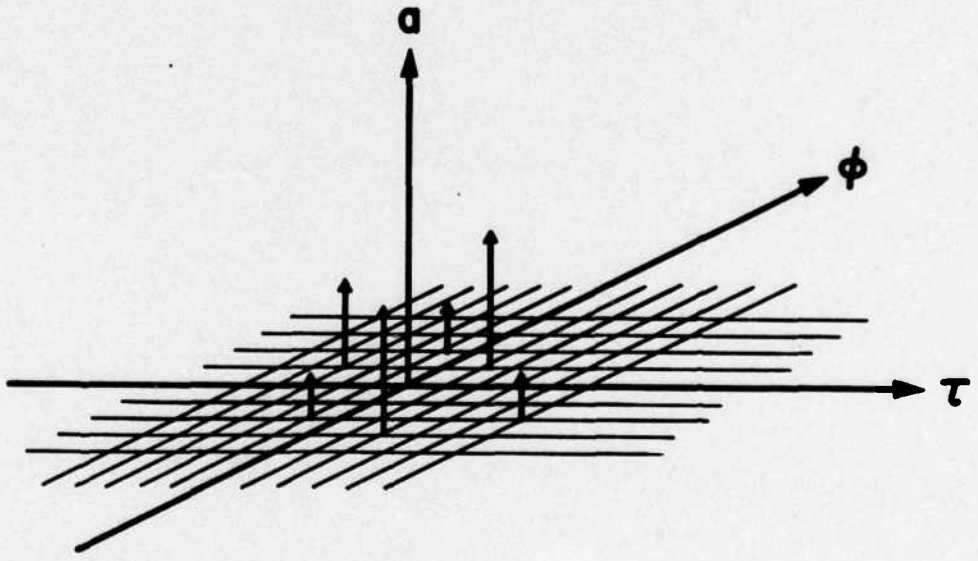

FIGURE 2. EXAMPLE OF SIGNAL SPREADING FUNCTION

constant with range over a pulse length. The doppler spread of the scatterers is assumed zero, since scatterer doppler spreading is typically much smaller than LFM bandwidths and hence, would have negligible effect anyway. If the average spacing of the scatterers is small compared to the size of a range resolution cell for any bandwidths under consideration, then the reverberation appearing at the receiver input can, with the postulated model, be approximated with stationary gaussian noise having a power density spectrum equal to the energy density spectrum of the transmitted signals.

One of the things of interest in this study will be the effect on signal-to-noise and signal-to-reverberation performance of the variation of LFM pulse bandwidth (W) and pulse length (T). For this purpose it is assumed that background noise is white so that the noise power in the band of the signal is directly proportional to signal bandwidth. Furthermore, it is assumed that reverberation power at the input to the signal processor is directly proportional to pulse length. We also assume that receiver input reverberation level does not depend on the bandwidth of the transmitted signal.

DETECTION

The processor for the LFM waveform is a baseband I and Q correlator in which the received signals are correlated with a reference signal consisting of a delayed replica of the transmitted signal. See Figure 3. Correlations are computed at closely spaced intervals of delay over all delays for which significant signal returns are expected. In addition, an integrator is included to combine returns that would normally appear at the correlator output at different resolvable times, due to range and doppler spreading of the echo. Results are obtained both with and without the use of the integrator.

Figure 4 shows the correlator output waveform for the case of three paths distributed as shown in range and doppler. This illustrates the well known range-doppler ambiguity of LFM. The path that is doppler shifted appears at the correlator output with a shift in time compared to where it would appear if its doppler were zero. In fact it may be shown that if the doppler shift is much less than the pulse bandwidth, a signal with an equivalent time delay τ_e and zero doppler will produce the same correlator output waveform as a signal with an actual delay τ and doppler ϕ, where

$$\tau_e = \tau + \frac{T}{W}\phi, \qquad \phi << W$$

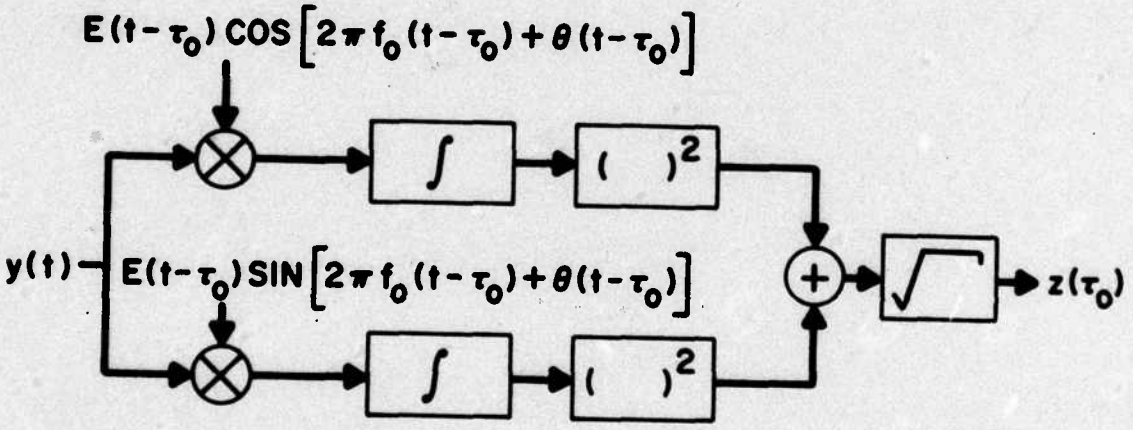

$$y(t) = \sum_{i=1}^{N} a_i E(t-\tau_i)\cos\left[2\pi f_0(t-\tau_i) + 2\pi\phi_i t + \theta(t-\tau_i)\right]$$

FIGURE 3. BLOCK DIAGRAM OF CORRELATOR

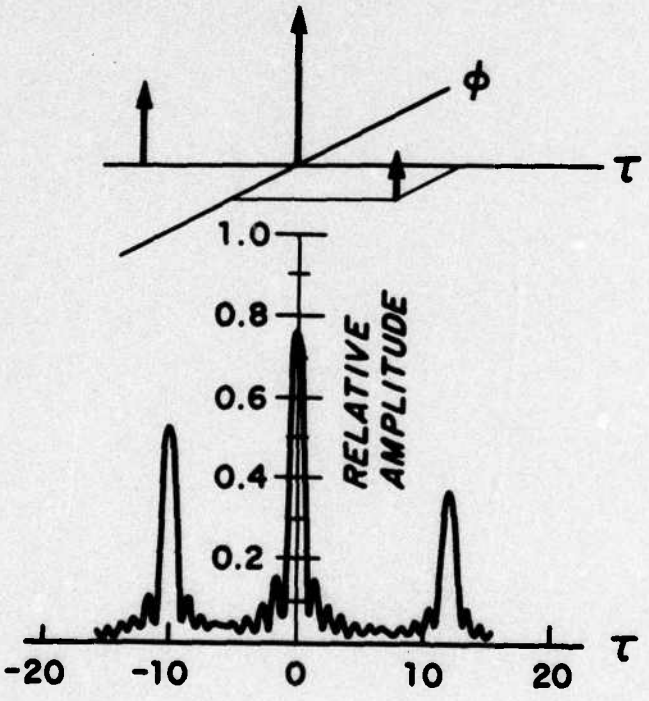

FIGURE 4. CORRELATOR OUTPUT FOR THREE PATHS

Furthermore, with our spreading model, in which range delay and doppler shift are independent gaussian random variables, a signal with multiple arrivals spread in time only with standard deviation

$$\sigma_{\tau e} = \sqrt{\sigma_\tau^2 + (T\sigma_\phi/W)^2}$$

will produce the same results as a signal spread in both time and doppler having standard deviations σ_τ and σ_ϕ respectively. Thus, in this study, it was not considered necessary to treat time spreading and doppler spreading as separate effects. Hence, doppler spread has been assumed zero for all results that will be shown.

Figure 5 shows correlator output waveforms for six successive pings all from the same population, for the case

$WT = 50$

$N = 6$ paths

$\sigma_\tau = 2/W$

$\sigma_a = 3$ db

$\sigma_\phi = 0$ Hz

In each ping, the amplitudes of the individual arrivals are normalized such that the total energy (sum of the square of the amplitudes) is constant. If all of the energy were concentrated in a single arrival, the correlator output would peak at the level marked "theoretical maximum". Notice that the peaks are somewhat reduced from the theoretical maximum and there are usually several peaks.

When dealing with discrete numbers of arrivals, it is helpful to be aware of the denseness with which these arrivals are "packed" relative to the time resolution of the signal. For time delays distributed normally about a mean $\bar{\tau}$, the densest packing will occur, on the average over many pings, in the time resolution cell centered on $\bar{\tau}$. We will define a quantity, η, to be a measure of the denseness:

$$\eta = NE\left[\frac{\text{peak correlator output for } \tau_o = \bar{\tau}}{\text{theoretical maximum correlator output peak}}\right]$$

This can be shown to be equal to, for $\phi = 0$

$$\eta = \int_{-\infty}^{\infty} \left|A(\tau-\tau_o, 0)\right|^2 \; P[(\tau-\tau_o)/\sigma_\tau] \; d\tau$$

where

$E(X)$ = Expectation of X

$A(\tau,\phi)$ = Ambiguity function of the transmitted waveform

$P(x)$ = Zero mean gaussian probability density function with standard deviation of unity

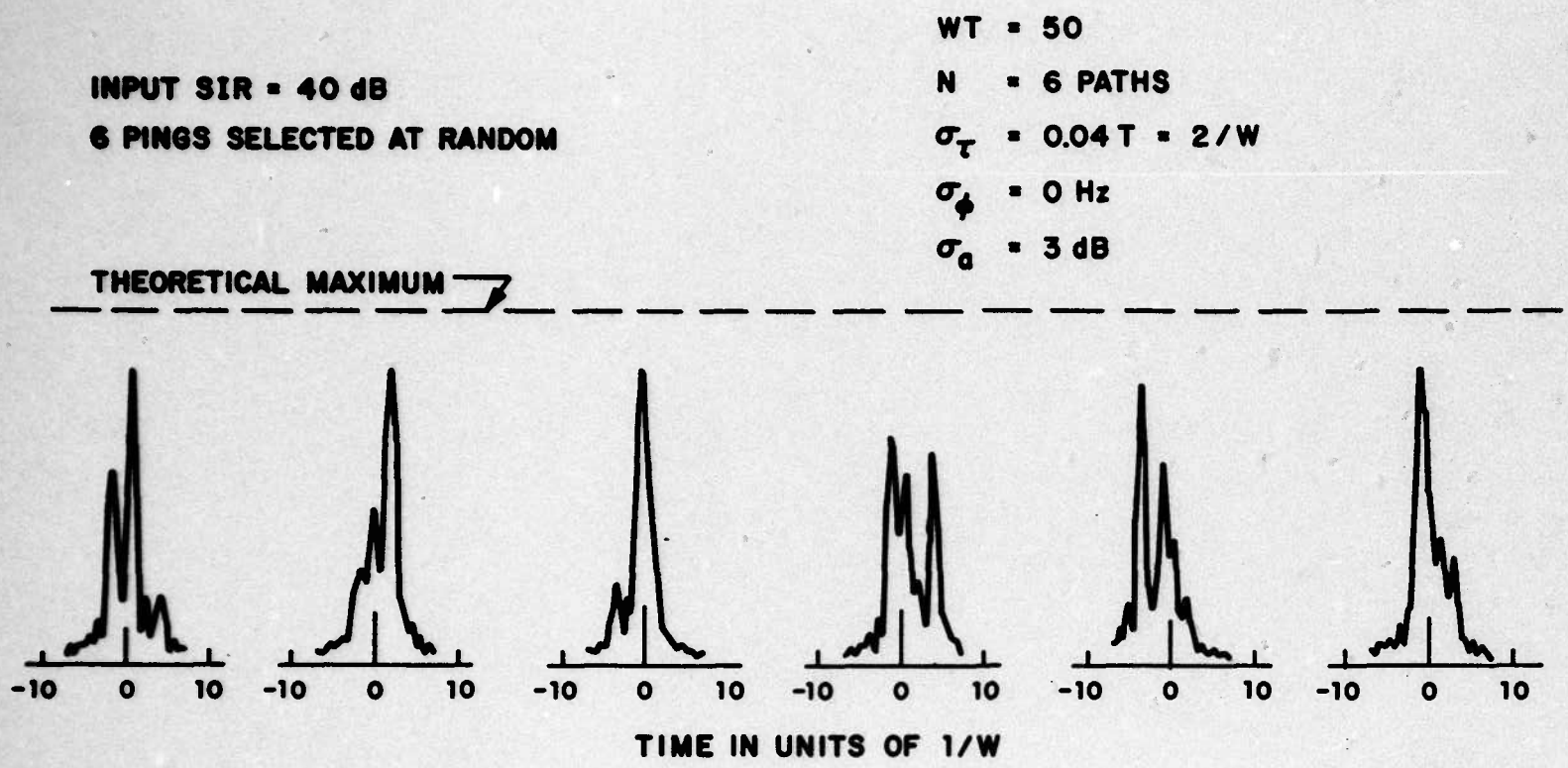

FIGURE 5. CORRELATOR OUTPUT WAVEFORMS

η/N is the fraction of signal energy, averaged over many pings, contributing to the correlator output at the reference delay, $\tau_o = \bar{\tau}$, most likely to produce a correlator peak. In other words, it is a measure of the signal energy contained within the particular range resolution cell which is most likely to contain the greatest signal energy. On the average, η is approximately equal to the number of arrivals that appear in this resolution cell. If $\eta<<1$, since we are dealing with discrete arrivals, the arrivals are distributed thinly among time resolution cells, and the correlator output will appear "spiky". If $\eta>>1$, corresponding to, on the average, many more than one arrival in one resolution cell, the output waveform will tend to be smoother.

In the results to be shown, we will see that the effect of over-averaging, or smoothing the correlator output is different depending on whether η is greater than or less than unity.

In the Monte Carlo procedure employed in this study, a detection is counted if the correlator output waveform exceeds the threshold at any time during the ping and that threshold crossing would not have occurred in the absence of the echo. The decision process is primarily sensitive to peaks of the output waveform. Thus, for example, if there are N arrivals, and $\eta<<1$ so that they are thinly distributed, the largest peak of the correlator output waveform will be caused by the arrival containing the most energy. If the energy were equally divided between all arrivals, then there would be N equal output peaks with an amplitude of $1/\sqrt{N}$ of the amplitude which would result if all the energy were contained within a single arrival. However, if the energy is distributed unequally among the N arrivals, as with our model, then, for any given ping, the arrival which contains the greatest energy will determine the detectability of that echo, all other arrivals contributing essentially nothing. Furthermore, the fraction of the total energy contained in this maximum arrival is always greater than 1/N. Hence, the detectability of signals consisting of multiple arrivals unequally distributed in energy can be expected to be better than the detectability of echos whose energy is equally divided among all arrivals. As we will see in the results to follow, the presence of multiple arrivals has a surprisingly small effect on detection, and the reason for this is in part the unequal division of energy between arrivals.

RESULTS

Results are shown in terms of the minimum detectable correlator input signal-to-interference ratio (SIR) required to produce, at the processor output, a detection probability of 0.5 when the output threshold is set for a false alarm probability of 0.01. Detection probability, as we have stated, is the probability that at least one threshold crossing will occur, on a given ping, with an echo present that would not have occurred with the echo absent. False alarm probability is the fraction of time, over all pings, that the correlator output voltage is above the threshold in the absence of signal. The input interference is measured in the band of the signal and can be interpreted as either reverberation or noise.

Let us look first at the effect of the number of paths, N. For this, σ_τ is held constant and N varied from 1 to 50. Figure 6 shows typical correlator output waveforms for:

$TW = 50$

$\sigma_\tau = 2/W$ sec

$\sigma_a = 6$ db

$\sigma_\phi = 0$ Hz

The waveform at the extreme left is for N = 1. With only a single arrival, the correlator peak achieves its theoretical maximum*. For N=3, we see two clearly resolved arrivals with reduced peaks. For N=6, we find three peaks and for N=12 four peaks. Note, though, that as N increases, the largest peak does not decrease substantially beyond N=6. This is due to (a) the effect previously discussed regarding the unequal splitting of energy among arrivals and that the greater N, the more likely the occurrance of relatively large peaks; and (b) the fact that the average energy in a resolution cell tends to approach a constant value as η becomes much greater than unity. Note also that the "spikiness" of the output waveform diminishes as N increases. From observing these waveforms, we would expect that detectability would be best for N=1, and diminish gradually as N increases. This is borne out in Figure 7 which shows minimum detectable input SIR (called SIR_{min}) vs N (solid line). SIR_{min} is -10.6 db for a single arrival and increases to about -6 db for N=50, a loss in detection of 4.6 db. The dashed curve shows the effect of smoothing the correlator output with an integrating filter whose impulse response is a rectangle of duration $2\sigma_\tau$ ($= 4/W$). We see that, although detectability is degraded somewhat by the smoothing for small N, where the arrivals are thinly spread, it is significantly improved for large N. In fact, the effect of the integrator is to render detectability almost constant at about -9 db for all N.

*The theoretical maximum is defined as the maximum correlator output voltage when there is no interference and when all signal energy is contained within a single resolution cell.

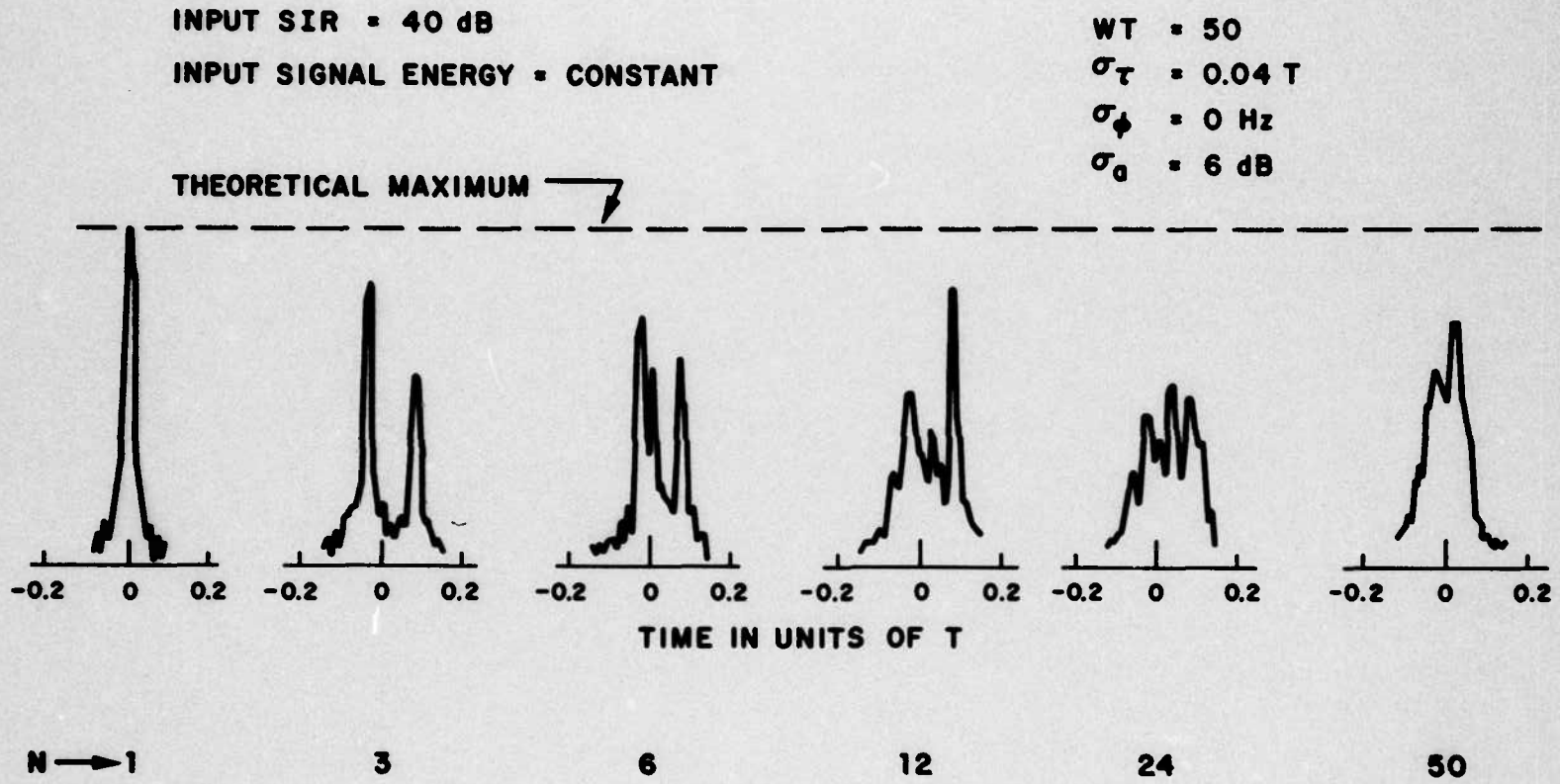

FIGURE 6. CORRELATOR OUTPUT WAVEFORMS vs NUMBER OF PATHS

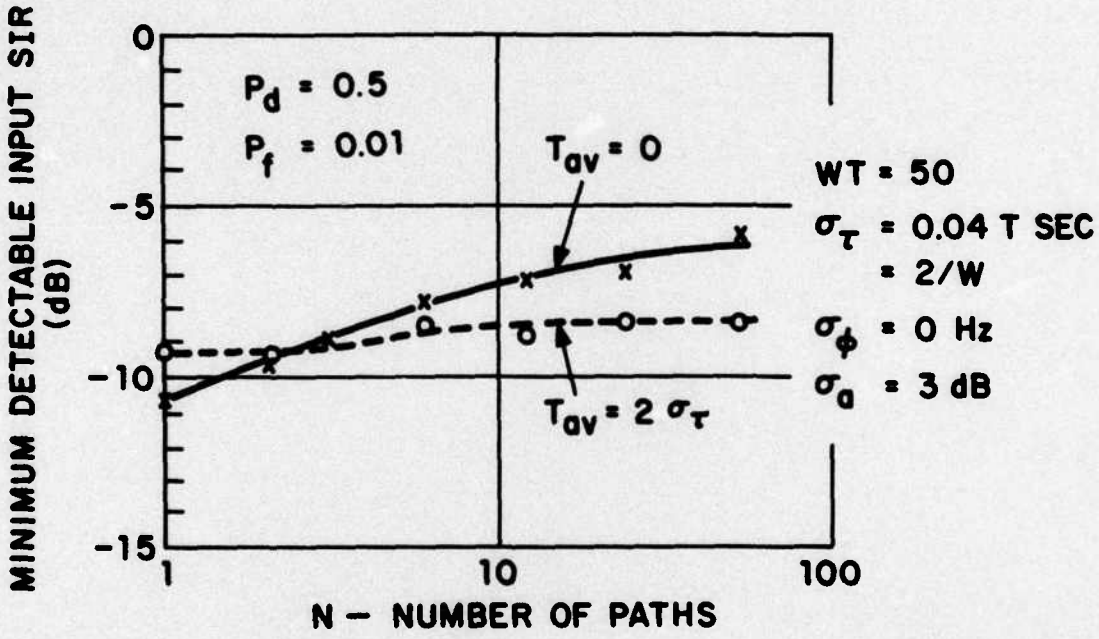

FIGURE 7. MINIMUM DETECTABLE INPUT SIR vs NUMBER OF PATHS

Now let us hold N constant at 50 and see the effect of varying the amount of spreading, σ_τ, again for WT=50. Typical correlator output waveforms are shown in Figure 8. For the first output waveform shown, $\sigma_\tau = .01/W$ which implies essentially no spreading at all and the correlator treats the echo as a single arrival. The second trace is for $\sigma_\tau = 1/W$ and some evidence of time spreading of the correlator output is evident, as well as some reduction in the peak. This trend continues as σ_τ increases. Note also the increase in "spikiness". We would expect detectability to diminish as σ_τ increases, and this is shown in Figure 9. The solid curve is a rough smoothing of the experimental points (X's). Detectability degrades (SIR_{min} increases) up to $\sigma_\tau = 5/W$, but then reverses, unexpectedly, for $\sigma_\tau = 10/W$. The cause of this reversal is not well understood. It is a consequence of our choice for detection probability of 0.5. If a higher detection probability of say 0.9 were chosen, this reversal would not have occurred. Nevertheless, the greatest loss in detectability for the range of σ_τ from 0 to 10/W is only about 5 db. Furthermore, with over-averaging of the correlator by an amount $2\sigma_\tau$, the greatest loss is only about 3 db. This comparison is a little bit unfair, because, in practice, we cannot predict the amount of spreading and hence, cannot match the amount of over-averaging to the spreading. However, detectability is a slowly varying function of averaging time, as is suggested in Figure 10 which shows SIR_{min} vs averaging time for $\sigma_\tau = 5/W$ and N=1 and 30. For 30 arrivals, the best detection is obtained with an integration time approximately equal to $2\sigma_\tau$. However, detection is only, at the most, 2 db worse for no integration. The curve for N=1 illustrates what can happen if the integration time is too long. For N=1, of course, the best detection is obtained with no integration. However, if we over-average by as much as 10 range resolution cells, the loss in detectability is less than 2 db. Beyond this point, however, the losses begin to increase rather rapidly.

One of the most important questions that we are attempting to answer in this study is: How should echo energy splitting effect the choice of the transmitted signal bandwidth, W, and the transmitted pulse length, T? Were it not for energy splitting, to obtain maximum detection performance, it would be best to use all the bandwidth available when reverberation limited and all the pulse length (transmission time) available when noise limited. There are other constraints on these parameters, however. Available bandwidth is limited by the efficient bandwidth of the projector and the need for multiple frequency channels. Transmission time is limited by the need to cover a wide search and by the non-stationarity of reverberation during a ping cycle. Our concern, then, is whether the environment will place

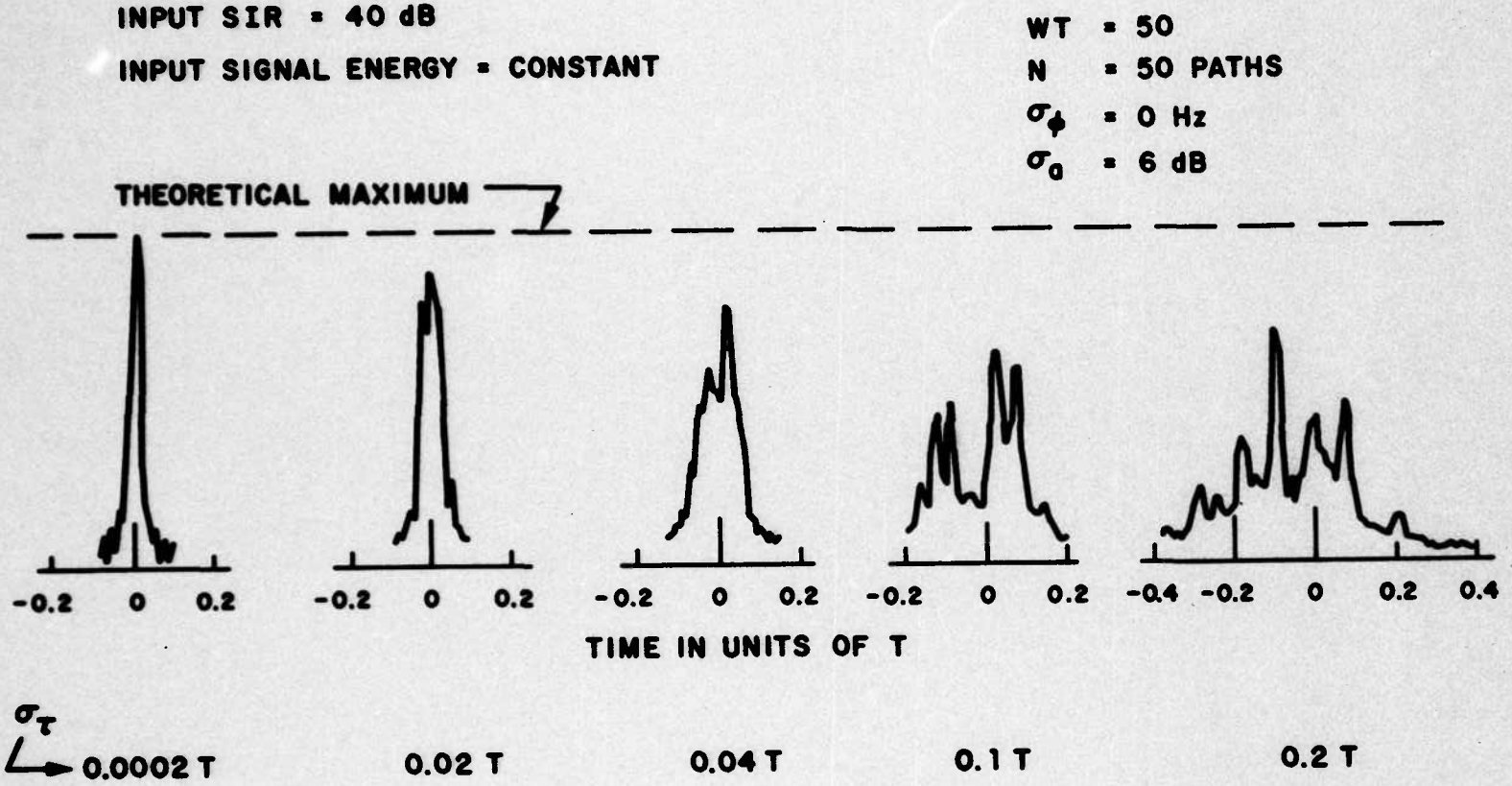

FIGURE 8. CORRELATOR OUTPUT WAVEFORMS vs TIME SPREADING

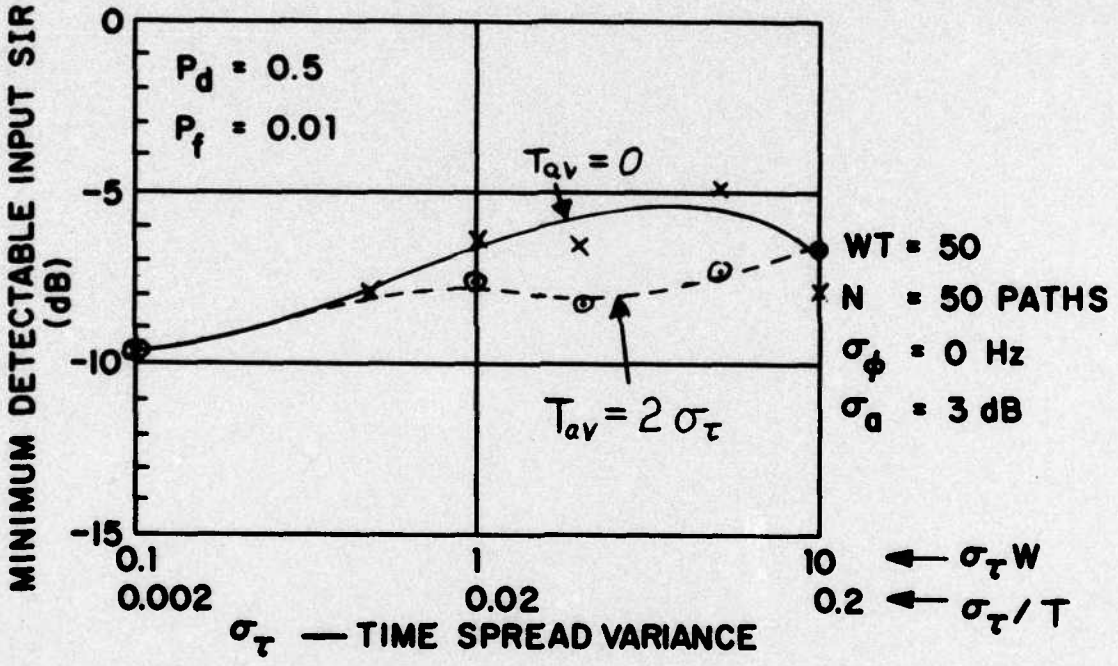

FIGURE 9. MINIMUM DETECTABLE INPUT SIR vs TIME SPREADING

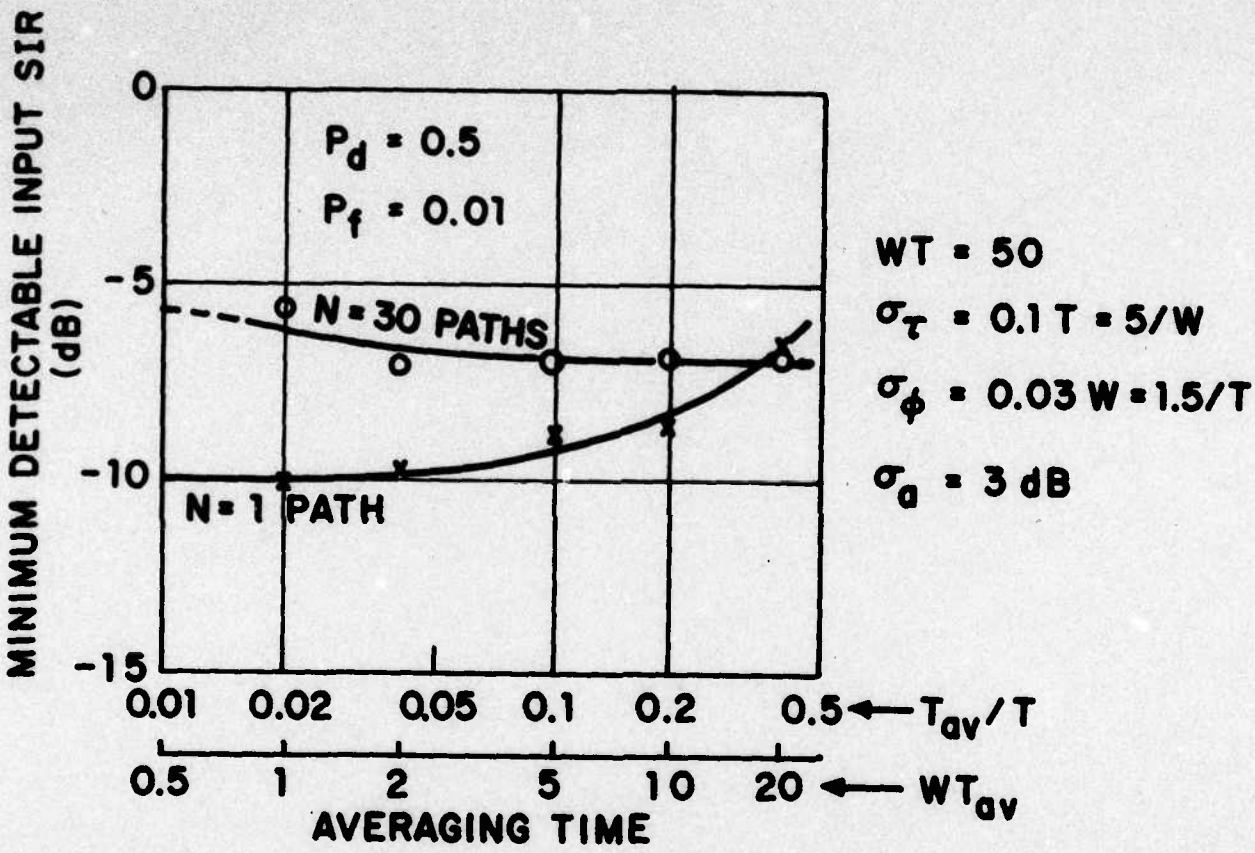

FIGURE 10. MINIMUM DETECTABLE INPUT SIR vs AVERAGING TIME

constraints on the choice of W and T that are more stringent than these other constraints. The following results provide some insight into this question.

Figure 11 shows correlator output waveforms for four different transmitted signal bandwidths. The number of arrivals, N, is 50 and they are spread in time delay by $\sigma_\tau = .04T$. The first waveform is for $W = 10/T$ ($\sigma_\tau W = .4$) and we see that all of the 50 paths fall within a single range resolution cell and the correlator output achieves its theoretical maximum value. As bandwidth is increased, the width of a range resolution cell becomes smaller and more evidence of energy splitting is observed. Hence, we would expect that the performance at the wider bandwidths would be degraded from theoretical performance more than it would at the narrower bandwidths. This is seen in Figure 12, which shows SIR_{min} vs signal bandwidth. The lower curve, labeled $\sigma_\tau = 0$, is the "theoretical" curve for no energy splitting. This curve has the expected slope of 10 db per decade reflecting the well known relationship between the input and output signal-to-noise ratio of a correlator:

$$\text{output SNR} = K \cdot WT \cdot \text{input SNR}$$

where K is a constant and the ratios are power ratios. The upper curve of Figure 12 is for the spreading conditions described above. We see that the loss due to spreading (the vertical distance between curves) varies between 2 and 5 db, and does not appear to increase very much with increasing bandwidth. As a matter of fact it decreases slightly at the extreme bandwidths. This is the same effect as noted above with large values of σ_τ. The largest TW in Figure 12 is 250, for which $W\sigma_\tau = 10$.

What does this say about how much bandwidth to use? The important parameter in assessing the performance of signals and processors is not minimum detectable input signal-to-interference ratio, as we have been using, but rather <u>minimum detectable input signal level</u>. For discussions thus far the two are equivalent since no parameters have been varied that effect input interference level. When bandwidth is a parameter, one must account for the fact that, under the assumption of white noise, the interference power level, when noise limited, is directly proportional to bandwidth.

Thus, from Figure 12, two curves are derived showing minimum detectable input signal vs W for noise limited and for reverberation limited conditions. These are shown in Figure 13. Now we can judge the effects on detection of employing wide bandwidth. When reverberation limited, the wider bandwidths are clearly better

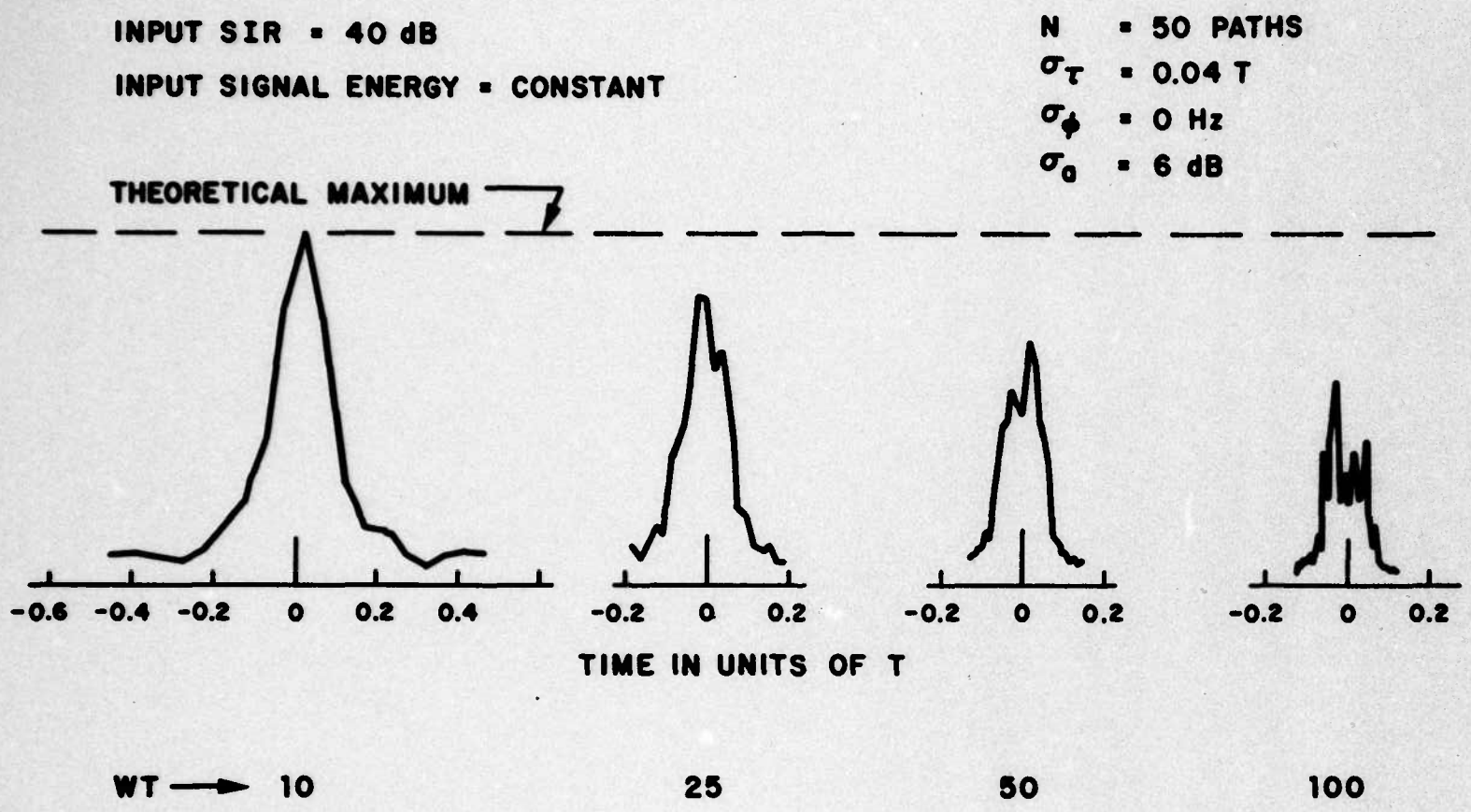

FIGURE 11. CORRELATOR OUTPUT WAVEFORMS vs PULSE BANDWIDTH

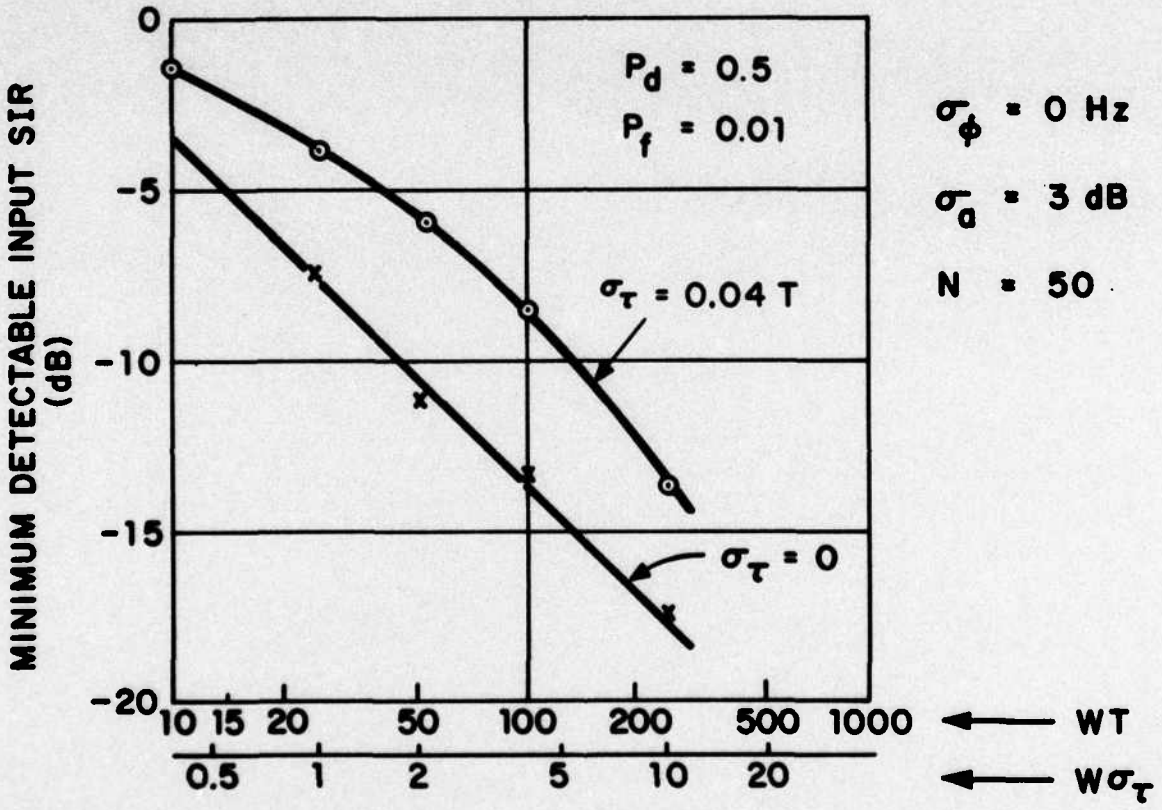

FIGURE 12. MINIMUM DETECTABLE INPUT SIR vs PULSE BANDWIDTH

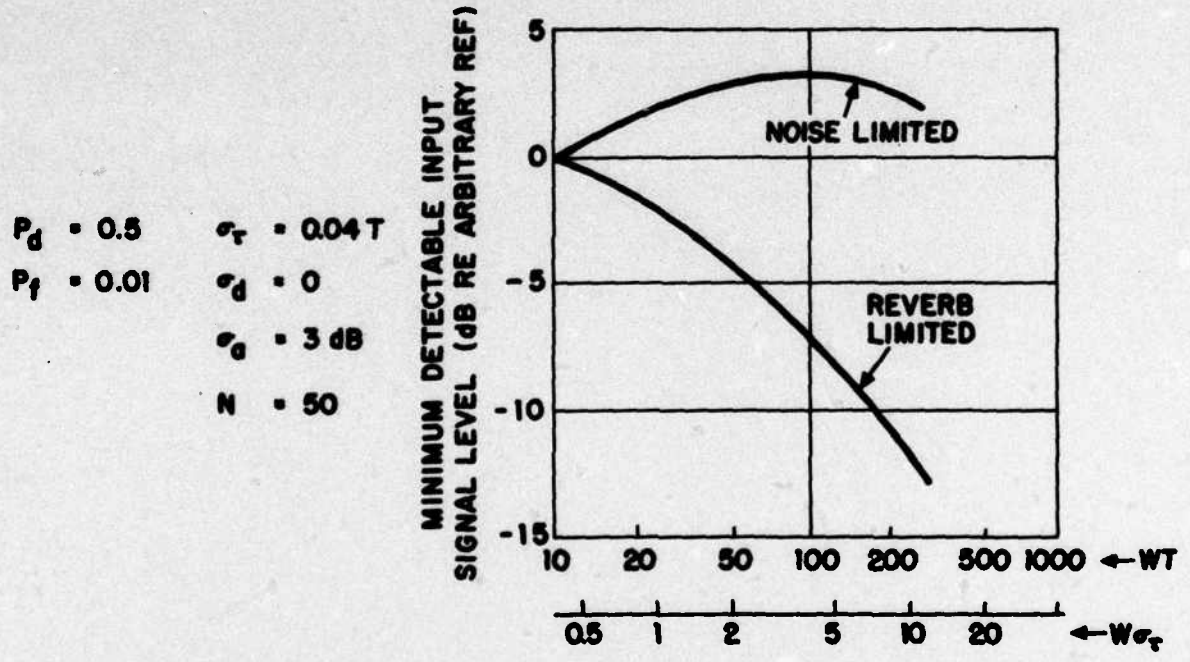

FIGURE 13. MINIMUM DETECTABLE INPUT SIGNAL LEVEL vs BANDWIDTH

than the narrower bandwidths. For WT = 100, reverberation limited performance is about 5 db better than for WT = 20. When noise limited however, some loss in performance is incurred at the wider bandwidths. For WT = 100, noise limited performance is about 2 db poorer than for WT = 20.

These results by themselves are not conclusive. We have used only one value of signal spreading (σ_τ = .04T) and, for that matter, only one spreading model. In addition, we have selected only one output criterion: p_d = .5, p_f = .01. However, these results are encouraging. They appear to be telling us that even in the presence of signal spreading, wide pulse bandwidth can buy significant reverberation limited performance at the cost of only a small degradation in noise limited performance.

In reference 2, similar results are obtained for a spreading model in which signal energy is spread uniformly in range and doppler and the correlator output is integrated uniformly over the spread. For an LFM waveform with time spreading of 5 range resolution cells (corresponding approximately to $W\sigma_\tau$ = 10 for the random spreading model), reverberation limited performance is only about 2 db worse than theoretical -- a strong justification for the use of wide bandwidths.

CONCLUSIONS

1. Echo detectability is a function, not only of the number of resolution cells over which signal energy is spread but also of the number of individual discrete arrivals within a ping. Detectability also depends on the expected spread in amplitudes of the individual arrivals, being better with more amplitude spread.

2. For choices of bandwidths usually available in long range active sonar systems, echo energy splitting does not appear to cause a serious limitation and, to attain the best possible echo detectability under reverberation limited conditions, one should use as much bandwidth as possible.

3. Over-averaging the correlator output provides modest gains in detection performance when signal energy spreading is dense ($\eta>1$). However, when signal energy is thinly spread ($\eta<1$), it is better <u>not</u> to over-average the correlator output.


ND
ATE

As we will see in the results to follow, the presence of multiple arrivals has a surprisingly small effect on detection, and the reason for this is in part the unequal division of energy between arrivals.